Published in "Langmuir 34(10): 3215–3220, 2018"
which should be cited to refer to this work.

Synthesis and Biophysical Characterization of an Odd-Numbered 1,3-Diamidophospholipid

Frederik Neuhaus,[†,‡] Dennis Mueller,[†] Radu Tanasescu,[†] Sandor Balog,[§] Takashi Ishikawa,[∥] Gerald Brezesinski,[⊥] and Andreas Zumbuehl*[,†,‡]

[†]Department of Chemistry, University of Fribourg, Chemin du Musée 9, 1700 Fribourg, Switzerland
[‡]National Centre of Competence in Research in Chemical Biology, Quai Ernest Ansermet 30, 1211 Geneva, Switzerland
[§]Adolphe Merkle Institute, University of Fribourg, Chemin du Verdiers 4, 1700 Fribourg, Switzerland
[∥]Paul Scherrer Institute (PSI), OFLB/010, 5232 Villigen PSI, Switzerland
[⊥]Max Planck Institute of Colloids and Interfaces, Research Campus Potsdam-Golm, 14476 Potsdam, Germany

S *Supporting Information*

ABSTRACT: Nanomedicine suffers from low drug delivery efficiencies. Mechanoresponsive vesicles could provide an alternative way to release active compounds triggered by the basic physics of the human body. 1,3-Diamidophospholipids with C16 tails proved to be an effective building block for mechanoresponsive vesicles, but their low main phase transition temperature prevents an effective application in humans. As the main phase transition temperature of a membrane depends on the fatty acyl chain length, we synthesized a C17 homologue of a 1,3-diamidophospholipid: Rad-PC-Rad. The elevated main phase transition temperature of Rad-PC-Rad allows mechanoresponsive drug delivery at body temperature. Herein, we report the biophysical properties of Rad-PC-Rad monolayer and bilayer membranes. Rad-PC-Rad is an ideal candidate for advancing the concept of physically triggered drug release.

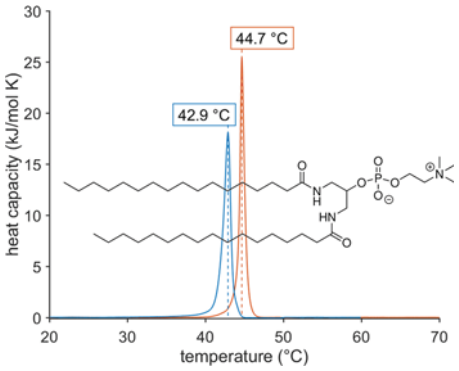

INTRODUCTION

The emerging field of mechanoresponsive drug delivery seeks to harness changes in physics between the healthy and diseased tissues as triggers for targeting drugs to the place where they are needed.[1−3] One interesting trigger is the shear force in blood vessels: following Murray's law, this force is balanced below 1.5 Pa throughout the entire vascular system to minimize the work needed to transport blood in the body.[4,5] At the site of a stenosis, the shear force is at least ten times higher[6,7] and this change in force might be used to activate drug release from either nanoparticle aggregates[8] or lenticular vesicles.[3]

Compared to the natural phospholipid 1,2-dipalmitoyl-*sn*-glycero-3-phosphocholine (DPPC, **1** see Figure 1), the 1,3-diamidophospholipid 1,3-palmitoylamido-1,3-deoxy-*sn*-glycero-2-phosphatidylcholine (Pad-PC-Pad, **2**) features two major differences: (i) the fatty acyl esters are replaced with amide moieties capable of forming intermolecular H-bonding networks.[9,10] (ii) The non-natural 1,3-arrangement is spacing the tails apart, leading to the bilayer membrane interdigitation.[10,11] The combination of these two effects leads to constrictions on the vesicle geometry, and lenticular or d-form shaped vesicles are formed.[12] These vesicles are tight when left untouched on the bench but release their cargo when they are mechanically stimulated, for example, by shaking. In other words, these vesicles are mechanoresponsive.

Although being self-assembled from the artificial phospholipid Pad-PC-Pad (**2**),[3] the vesicles were found to be surprisingly nontoxic and were not activating the complement system in *in vivo* experiments.[13,14] Therefore, Pad-PC-Pad (**2**) vesicles might be ideal candidates for mechanoresponsive vesicular drug delivery. However, the main phase transition of Pad-PC-Pad (**2**) lies at T_m = 37 °C, and heating the vesicles to this temperature will lead to the immediate full release of any vesicle-entrapped cargo because of the leakiness of a liquid-crystalline membrane[10] and the leakiness of a lipid membrane close to the chain-melting regime.[15] It was therefore necessary to increase the T_m of the membrane while maintaining the mechanosensitivity. A straightforward solution is to formulate vesicles from the C18 analogue[16] of Pad-PC-Pad (**2**), termed Sad-PC-Sad (**3**). Vesicles of Sad-PC-Sad (**3**) showed a T_m = 52 °C, but unfortunately, the mechanoresponsiveness of the vesicles at room temperature was lost.[10] Therefore, we have now synthesized and characterized the C17 analogue of Pad-PC-Pad (**2**). The correct term for a C17 fatty acid is margaric acid and its abbreviation, M, is more typically associated with myristic acid.[17] This is the reason why we have chosen a letter

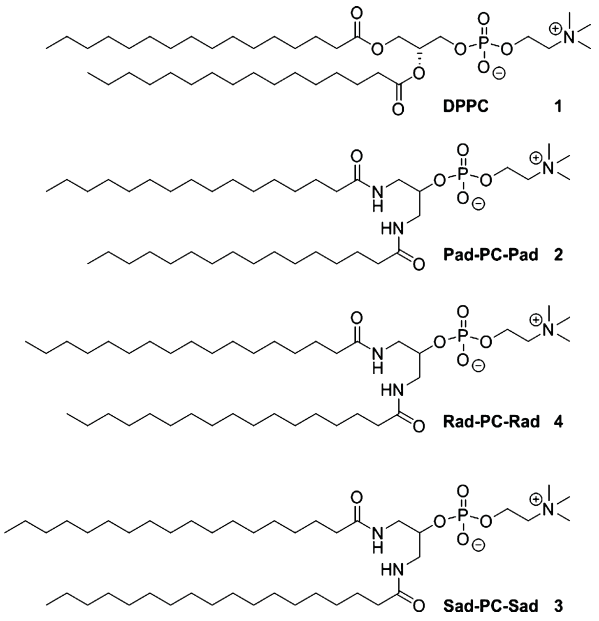

Figure 1. Schematic depiction of the natural phospholipid DPPC and the 1,3 diamidophospholipids with C16 (Pad-PC-Pad), C17 (Rad-PC-Rad), or C18 (Sad-PC-Sad) fatty acyl chains.

between P(almitoyl) and S(tearoyl) and named the molecule described in this paper Rad-PC-Rad (**4**).

In this publication, we discuss the synthesis and the characterization of Rad-PC-Rad (**4**) monolayers and bilayers and demonstrate that Rad-PC-Rad (**4**) vesicles are ideal candidates for further research into mechanoresponsive drug delivery.

RESULTS AND DISCUSSION

Synthesis. The 1,3-diamidophospholipid Rad-PC-Rad (**4**) has been synthesized expanding from our previously reported synthetic route (see Scheme 1 and Supporting Information).[3] The substitution of phosphorus oxytrichloride with 1,3-dichloropropanol led to a phosphorochloridate. The second substitution with Boc-protected ethanolamine led to the reasonably stable phosphoramidate **5**. This intermediate was transformed into a diazide, followed by a reduction to the diamine. The heptadecanoyl chains were accessed via heptadecanoic acid chloride (**6**) prepared from heptadecanoic acid with thionyl chloride and were reacted with the diamine to yield headgroup-protected phosphoramidate **7**. The final diamidophospholipid Rad-PC-Rad (**4**) was reached after acidic headgroup deprotection and quaternization with dimethyl sulfate. The overall yield after five steps was 37% starting from the headgroup-protected dichloropropyl phosphoramidate **5**. The chemically pure diamidophospholipid Rad-PC-Rad (**4**) was then characterized on a molecular level, as monolayers at the air–water interface [two-dimensional (2D) model] and as bulk systems (three-dimensional model).

Surface Pressure/Area per Molecule Isotherms. The surface pressure/area per molecule isotherm measurements were carried out on a Langmuir–Pockels trough, equipped with a Wilhelmy paper balance (accuracy 0.2 mN/m), at the air–water interface. The isotherms were measured at different subphase temperatures between 5 and 25 °C (see Figure 2).

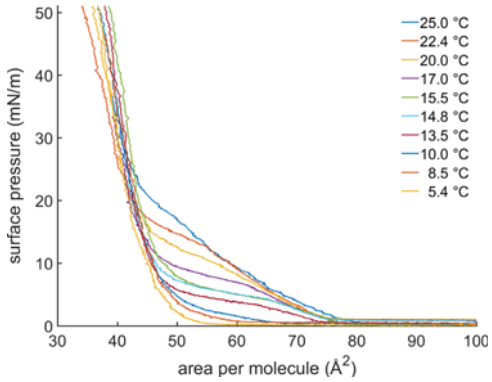

Figure 2. : Surface pressure/area per molecule isotherms of a Rad-PC-Rad (**4**) monolayer at the air–water interface on a Langmuir–Pockels trough with an aqueous subphase at different temperatures. The surface pressure was recorded via a Wilhelmy paper balance (accuracy 0.2 mN/m).

Rad-PC-Rad (**4**) monolayers showed a typical liquid-expanded (LE) to liquid-condensed (LC) phase behavior. Above 10 °C, the plateau of an expanded/condensed phase coexistence was observed. The appearance of the plateau is accompanied by a shift of the initial lift-off area per molecule to higher values. The plateau represents the first-order phase transition from a LE to LC phase. As observed for several diamidophospholipids, the plateau is not fully horizontal, especially it becomes steeper as the temperature increases.[9] The monolayers themselves are stable over the measurable

Scheme 1. Synthesis of Rad-PC-Rad (4) Starting from Dichloridate 5, Adding the Odd-Numbered Fatty Acid Chain Heptadecanoic Acid Chloride (6) Followed by the Deprotection and Quaternization of Intermediate 7

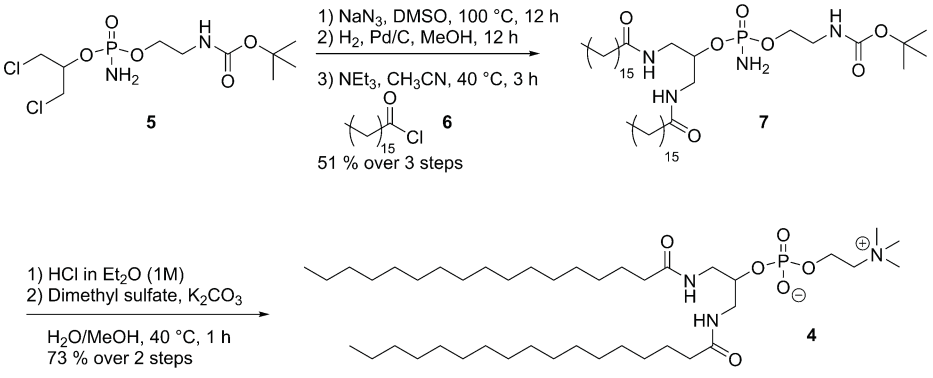

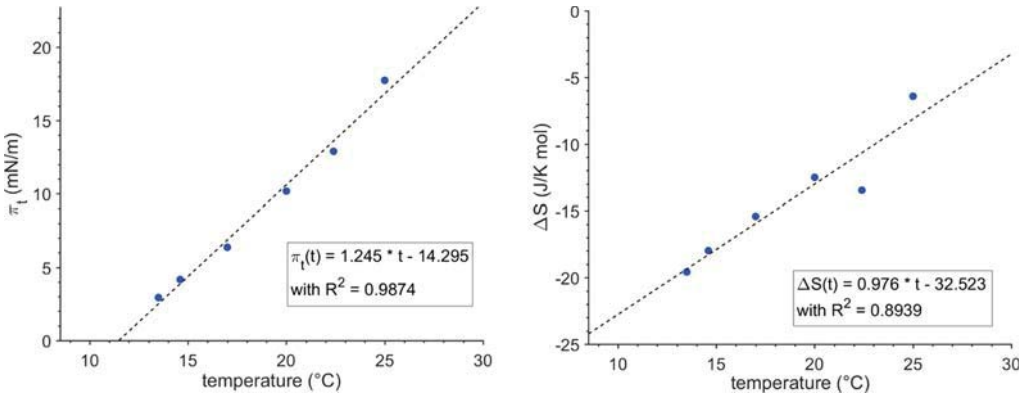

Figure 3. Temperature dependence of the main phase transition pressure π_t (left) and temperature dependence of the entropy change (ΔS) (right) at the main phase transition of Rad-PC-Rad (**4**) monolayers spread at the air−water interface.

Table 1. Summarized Data from GIXD Measurements of Rad-PC-Rad (4) Monolayers at Different Temperatures and Surface Pressures[a]

T/°C	π/mN/m		degen.	non-degen.	a	b	c	α/deg	β/deg	γ/deg	dist	τ/°	A_{xy}/Å^2	A_0/Å^2
10	30	Q_{XY}	1.34	1.45	5.57	5.15	5.15	114.5	122.8	122.8	0.108	38.0	24.1	19.0
		Q_Z	0.88	0.00							NN	NN		
15	30	Q_{XY}	1.36	1.47	5.51	5.09	5.09	114.4	122.8	122.8	0.109	35.7	23.6	19.1
		Q_Z	0.82	0.00							NN	NN		
20	14	Q_{XY}	1.34	1.47	5.61	5.11	5.11	113.4	123.3	123.3	0.127	35.8	24.0	19.4
		Q_Z	0.81	0.00							NN	NN		
	18	Q_{XY}	1.36	1.47	5.50	5.08	5.08	114.4	122.8	122.8	0.109	34.7	23.5	19.3
		Q_Z	0.79	0.00							NN	NN		
	22	Q_{XY}	1.37	1.47	5.47	5.06	5.06	114.6	122.7	122.7	0.105	33.9	23.3	19.3
		Q_Z	0.77	0.00							NN	NN		
	26	Q_{XY}	1.38	1.47	5.36	5.04	5.04	115.7	122.1	122.1	0.084	32.9	22.9	19.2
		Q_Z	0.76	0.00							NN	NN		
	36	Q_{XY}	1.43	1.48	5.13	4.95	4.95	117.7	121.1	121.1	0.046	27.1	21.7	19.3
		Q_Z	0.63	0.00							NN	NN		
30	26	Q_{XY}	1.37	1.47	5.46	5.07	5.07	114.8	122.6	122.6	0.101	29.2	23.3	20.3
		Q_Z	0.64	0.00							NN	NN		
	34	Q_{XY}	1.38	1.47	5.41	5.05	5.05	115.2	122.4	122.4	0.094	28.8	23.1	20.2
		Q_Z	0.64	0.00							NN	NN		

[a] A_{xy}: in-plane area per chain and A_0: cross-sectional area per chain with $A_0 = A_{xy} \cos \tau$.

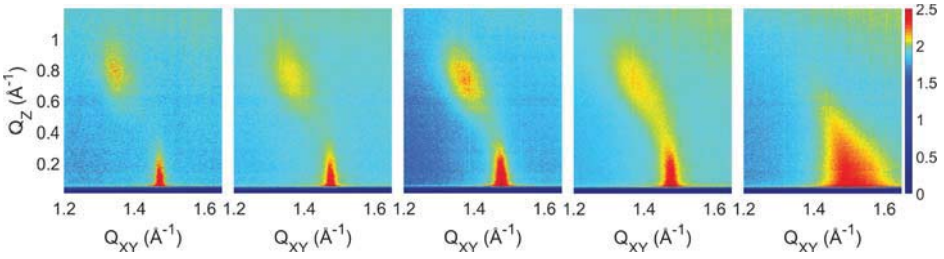

Figure 4. GIXD heatmaps of the diffraction intensities as a function of the in-plane Q_{XY} and out-of-plane Q_Z components of the scattering vector Q for Rad-PC-Rad (**4**) at 20 °C and different surface pressures π (from left to right: 14, 18, 22, 26, and 36 mN/m).

range of surface pressures up to an instrument-based cutoff at 51 mN/m. From the onset of the plateau, it is possible to determine the temperature-dependent main transition pressure π_t. For Rad-PC-Rad (**4**), this dependence can be described by a linear function (see Figure 3).[18] The experimental data only deviate from this linear function in close vicinity of the minimum transition temperature T_0 below which the transition into a condensed phase directly starts from the gas-analogue state (resublimation process). For Rad-PC-Rad (**4**), this temperature is 11 °C. The temperature can be compared to the lift-off temperatures of the main phase transition of homologous 1,3-diamidophospholipids, showing a linear trend of T_0 versus the chain length (see Figure S14) because T_0 of the C16 homologue (**2**) is 1.3 °C and that of the C18 homologue (**3**) is 18 °C.[9]

From the area per molecule at the onset of the first-order phase transition (A_0) at π_t and the area at the end of the expanded−condensed phase coexistence (A_c), it is possible to calculate the enthalpy change (ΔH) of the phase transition using a modified 2D Clausius−Clapeyron equation.

$$\Delta H = (A_c - A_0)T \frac{d\pi_t}{dT}$$

With this, the entropy change dependency is represented by $\Delta S = \Delta H/T$ which is shown in Figure 3. The extrapolation of ΔS to zero gives the critical temperature of Rad-PC-Rad (**4**) monolayers of 33 °C. Above this temperature, no compression of the monolayer to a condensed state is possible. Compared to the critical temperatures of Pad-PC-Pad (**2**) (27 °C) and Sad-PC-Sad (**3**) (41 °C),[9] Rad-PC-Rad (**4**) fits well into the trend of an increasing critical temperature with increasing chain length.

Grazing Incidence-Angle X-ray Diffraction. Grazing incidence-angle X-ray diffraction (GIXD) experiments provide insights into the lattice structure of condensed monolayers on the Ångstrom scale.[19−23] The in-plane component of the scattering vector (Q_{XY}) and out-of-plane component (Q_Z) maxima of different measurements are presented in Table 1, and exemplary heatmaps are shown in Figure 4 (for the remaining heatmaps, see Supporting Information). For Rad-PC-Rad (**4**), two Bragg Peaks have been observed for every measured temperature/surface pressure combination. The signal at higher Q_Z is a degenerated signal composed of two equal signals. The Rad-PC-Rad (**4**) monolayers adopt an orthorhombic lattice structure described by a distorted rectangular unit cell, with a distortion in the NN (nearest neighbor) direction and a fairly high tilt angle t (between 27° and 36°) of the lipid tails tilted to the same NN direction. At 20 °C, the chain cross-sectional area (A_0) is around 19.3 Å^2, and therefore only marginally larger than that observed at lower temperatures (19.0 Å^2 at 10 °C and 19.1 Å^2 at 15 °C). This is a typical value for chains in a herringbone packing mode. This packing mode is supported by the distortion value obtained by extrapolation of the distortion versus $\sin^2(t)$ (see Figure S15).[15] d_0 amounts to -7.75×10^{-2} and is clearly different from zero which would be expected if the tilt is the only source for lattice distortion. In the present case, the herringbone packing is an additional source and might be caused by a hydrogen-bonding network between the headgroups.

With increasing surface pressure, the tilt angle t decreases to 0.41° per mN/m (see Figure S16). Assuming a constant cross-sectional area in the condensed phase, the tilting phase transition pressure can be determined from a plot of $1/\cos(t)$ versus the lateral pressure. Extrapolation to $1/\cos(t) = 1$ yields a tilting pressure of 62.3 mN/m (see Figure S16). Such a phase transition would usually be characterized by a kink in the surface pressure/area isotherm as expected for a second-order phase transition.[19] However, the expected transition surface pressure is too high to be observed with the used setup. The tilting phase transition pressure can be compared to those of other lipids, such as the C18-analogous diamidophospholipid Sad-PC-Sad (**3**). A trend is visible, with longer fatty acyl chains leading to higher tilting phase transition pressures.[9] At 30 °C, the cross-sectional area of Rad-PC-Rad (**4**) 20.2 Å^2 is in the expected range for rotator phases (for full data, see Table 1 as well as Figure 3 and Supporting Information).[9,24]

Cryo-Transmission Electron Microscopy. All cryo-transmission electron microscopy (cryo-TEM) images in this paper were measured according to a previously described protocol.[25] The cryo-TEM images recorded from large unilamellar vesicles (LUVs) entirely made of Rad-PC-Rad (**4**) show a significant number of strongly facetted shapes below the main phase transition temperature of the membranes ($T_m \approx 45$ °C, see below) (see Figures S10 and S11). In the previous work, we studied this in depth and depicted interleaflet chain interdigitation and hydrogen-bond networks as the main driving forces for this behavior.[10,26] The ratio between facetted and spherical vesicles calculated from Figure S10 is 21:4. The still occurring spherical shape might be due to small impurities in the prepared lipid membranes, as already small amounts of interface-active compounds can significantly influence the membrane shape and behavior.[27]

The interdigitation of the leaflets in a membrane can be directly measured from lateral cuts through the membrane in the cryo-TEM image (see Figure 5). To collect statistically

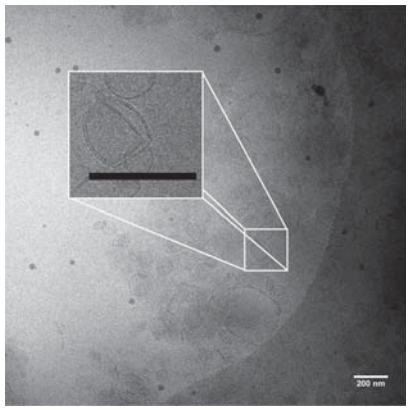

Figure 5. Cryogenic transmission electron micrograph of Rad-PC-Rad (**4**) vesicles and an inset of facetted vesicles. Both scale bars have a length of 200 nm (for additional cryo-TEM images, see Supporting Information).

relevant data, we measured 509 membrane cuts from Figure S10 (see Figure S12) with a mean membrane thickness of 3.20 ± 0.02 nm (N = 509). With two times 0.7 nm for the headgroups, the hydrophobic layer is 1.8 nm thick.[12] An all-trans alkyl chain of 16 C-atoms has a length of 2.05 nm.[28] Thus, the alkyl chains in a noninterdigitated bilayer would have a tilt angle of 64°, which is rather unlikely. Therefore, a full bilayer interdigitation can be assumed.

Differential Scanning Calorimetry. Interdigitation of the membrane leaflets also influences the membrane main-phase transition temperature.[29] In differential scanning calorimetry experiments from Rad-PC-Rad (**4**) containing LUVs with heating and cooling rates of 0.5 K/min, a main phase transition temperature of 44.7 °C with a change in enthalpy of 24.16 kJ/mol (see Figure S9) is observed. The main phase transition temperature is lower compared to a natural 1,2-diester phospholipid with margaric acid chains, which is 48.6 °C.[17] Also, the value for the bilayer main phase transition temperature is 11.5 K higher than the calculated critical temperature from the monolayer experiments. This corroborates that an additional attractive force needs to be overcome in bilayers which is not present in monolayers, most probably stemming from interdigitation.

As the main phase transition temperature of Rad-PC-Rad (**4**) containing vesicles is well above the human body temperature, these mechanosensitive liposomes are of interest for targeted drug release as described in the literature.[3,30] To investigate the potential of the liposomes in this regard, release experiments were carried out.

Release Experiments. Previously, we reported the 5(6)-carboxyfluorescein release from Pad-PC-Pad (**2**) containing

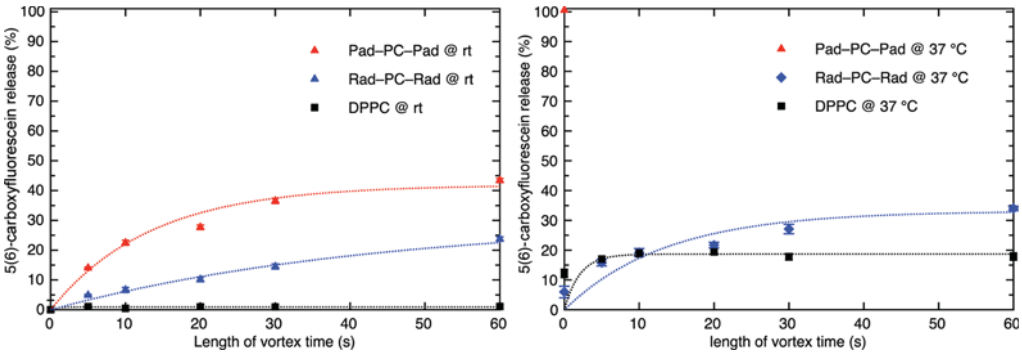

Figure 6. Release experiments using 5(6)-carboxyfluorescein-loaded Rad-PC-Rad (**4**) LUVs obtained via extrusion through a 100 nm track-edged filter membrane ($LUVET_{100}$). Triggered release was induced by shaking the samples for a specific amount of time on a vortex shaker. Pad-PC-Pad (**2**) at 37 °C showed an immediate full release of its cargo without shaking and was therefore only measured once.

vesicles. As Pad-PC-Pad (**2**) shows a strong spontaneous release already at temperatures slightly above its main phase transition temperature (T_m = 37 °C),[3] the use of this lipid at the average human body temperature of 37 °C[31] is not ideal. Increasing the T_m promises improved release properties. With the longer chain length compared to Pad-PC-Pad (**2**), Rad-PC-Rad (**4**) has a higher main phase transition temperature of 44.7 °C. This leads to a lower leakage of the vesicles at 22 °C (room temperature) as well as 37 °C (average human body temperature) (see Figure 6).

Each sample was treated with Triton X-100 to induce a full release of 5(6)-carboxyfluorescein.[3] At a temperature of 22 °C, Rad-PC-Rad (**4**) vesicles show a spontaneous release of 9% 5(6)-carboxyfluorescein after 7 days (see Figure S13), with a good mechanically induced release of 24% after 60 s of vortexing. Pad-PC-Pad (**2**) has a mechanically induced release of 44% after 60 s of vortexing, the release depends on the duration of vortexing with an immediate burst release and a slower continuous release afterward. It shows a spontaneous release of 15% after 7 days. DPPC (**1**) shows a mechanically induced release of 1% after 60 s vortexing and a spontaneous release after 7 days of 5%. At 37 °C, the mechanically induced release of Rad-PC-Rad (**4**) after 60 s of vortexing is 34%, whereas Pad-PC-Pad (**2**) shows 100% release without vortexing and DPPC (**1**) shows 18% release after 60 s of vortexing. These release experiments show the potential of Rad-PC-Rad (**4**) containing vesicles for targeted mechanoresponsive drug release at body temperature.

CONCLUSIONS

In conclusion, we reported the synthesis of a symmetrical 1,3-diamidophospholipid with C17 fatty acyl chains. The properties of the Rad-PC-Rad monolayers more closely resemble those of its C16 analogue compared to the C18 homologue. The bilayer membrane is interdigitated, and the vesicles are mildly faceted. The main phase transition temperature of 44.7 °C allows mechanoresponsive fluorescent cargo release at 37 °C, whereas the system remains stable at room temperature. Overall, Rad-PC-Rad is a promising system for advancing the concept of mechanoresponsive drug delivery. At temperatures of 20 °C and below, the molecules exhibit a herringbone packing mode in monolayers most probably caused by a hydrogen-bonding network between the headgroups. Surprisingly, this tight packing mode cannot be found at slightly higher temperatures (30 °C) at which the cross-sectional area (20.2 Å^2) indicates a rotator phase.

ASSOCIATED CONTENT

Supporting Information

The Supporting Information is available free of charge on the ACS Publications website at DOI: 10.1021/acs.langmuir.7b04227.

Synthesis, ^{1}H NMR, ^{13}C NMR of heptadecanoyl acid chloride (**6**); synthesis, ^{1}H NMR, ^{13}C NMR, and ^{31}P NMR of tert-butyl (2-((amino((1,3-diheptadecan-amidopropan-2-yl)oxy)phosphoryl)oxy)ethyl) and 1,3-diheptadecanamidopropan-2-yl (2-(trimethylammonio)-ethyl) phosphate (Rad-PC-Rad, **4**); differential scanning calorimetry; vesicle preparation; cryo-TEM images; release experiments; film balance measurements; and GIXD measurements (PDF)

AUTHOR INFORMATION

Corresponding Author

*E-mail: andreas.zumbuehl@unifr.ch.

ORCID

Frederik Neuhaus: 0000-0003-2749-7208
Sandor Balog: 0000-0002-4847-9845
Andreas Zumbuehl: 0000-0002-8003-4432

Notes

The authors declare no competing financial interest.

ACKNOWLEDGMENTS

Parts of this research were carried out at PETRA III at DESY, a member of the Helmholtz Association (HGF). The authors thank Dr. Uta Ruett and Dr. Florian Bertram for assistance in using beamline P08 and the Paul Scherrer Institut (PSI) Electron Microscopy (EM) facility for technical help. This work has been supported by the University of Fribourg and the Swiss National Science Foundation through a stipend professorship to A.Z. and through the National Centers of Competence in Research (NCCR) in Chemical Biology and Bio-inspired Materials.

REFERENCES

(1) Epshtein, M.; Korin, N. Shear targeted drug delivery to stenotic blood vessels. *J. Biomech.* **2017**, *50*, 217−221.

(2) Wang, J.; Kaplan, J. A.; Colson, Y. L.; Grinstaff, M. W. Mechanoresponsive materials for drug delivery: Harnessing forces for controlled release. *Adv. Drug Delivery Rev.* **2017**, *108*, 68−82.

(3) Holme, M. N.; Fedotenko, I. A.; Abegg, D.; Althaus, J.; Babel, L.; Favarger, F.; Reiter, R.; Tanasescu, R.; Zaffalon, P.-L.; Ziegler, A.;

Müller, B.; Saxer, T.; Zumbuehl, A. Shear-stress sensitive lenticular vesicles for targeted drug delivery. *Nat. Nanotechnol.* **2012**, *7*, 536−543.
(4) Murray, C. D. The Physiological Principle of Minimum Work: I. The Vascular System and the Cost of Blood Volume. *Proc. Natl. Acad. Sci. U.S.A.* **1926**, *12*, 207−214.
(5) Sherman, T. F. On connecting large vessels to small. The meaning of Murray's law. *J. Gen. Physiol.* **1981**, *78*, 431−453.
(6) Yin, W.; Shanmugavelayudam, S. K.; Rubenstein, D. A. 3D Numerical Simulation of Coronary Blood Flow and its Effect on Endothelial Cell Activation. *2009 Annual International Conference of the IEEE Engineering in Medicine and Biology Society*, 2009; pp 4003−4006.
(7) Holme, M. N.; Schulz, G.; Deyhle, H.; Weitkamp, T.; Beckmann, F.; Lobrinus, J. A.; Rikhtegar, F.; Kurtcuoglu, V.; Zanette, I.; Saxer, T.; Müller, B. Complementary X-ray tomography techniques for histology-validated 3D imaging of soft and hard tissues using plaque-containing blood vessels as examples. *Nat. Protoc.* **2014**, *9*, 1401−1415.
(8) Korin, N.; Kanapathipillai, M.; Matthews, B. D.; Crescente, M.; Brill, A.; Mammoto, T.; Ghosh, K.; Jurek, S.; Bencherif, S. A.; Bhatta, D.; Coskun, A. U.; Feldman, C. L.; Wagner, D. D.; Ingber, D. E. Shear-Activated Nanotherapeutics for Drug Targeting to Obstructed Blood Vessels. *Science* **2012**, *337*, 738−742.
(9) Fedotenko, L. A.; Stefaniu, C.; Brezesinski, G.; Zumbuehl, A. Monolayer properties of 1,3-diamidophospholipids. *Langmuir* **2013**, *29*, 9428−9435.
(10) Weinberger, A.; Tanasescu, R.; Stefaniu, C.; Fedotenko, I. A.; Favarger, F.; Ishikawa, T.; Brezesinski, G.; Marques, C. M.; Zumbuehl, A. Bilayer Properties of 1,3-Diamidophospholipids. *Langmuir* **2015**, *31*, 1879−1884.
(11) Serrallach, E. N.; Dijkman, R.; de Haas, G. H.; Shipley, G. G. Structure and Thermotropic Properties of 1,3-Dipalmitoyl-glycero-2-phosphocholine. *J. Mol. Biol.* **1983**, *170*, 155−174.
(12) Tanasescu, R.; Lanz, M. A.; Mueller, D.; Tassler, S.; Ishikawa, T.; Reiter, R.; Brezesinski, G.; Zumbuehl, A. Vesicle Origami and the Influence of Cholesterol on Lipid Packing. *Langmuir* **2016**, *32*, 4896−4903.
(13) Bugna, S.; Buscema, M.; Matviykiv, S.; Urbanics, R.; Weinberger, A.; Meszaros, T.; Szebeni, J.; Zumbuehl, A.; Saxer, T.; Müller, B. Surprising lack of liposome-induced complement activation by artificial 1,3-diamidophospholipids in vitro. *Nanomed. Nanotechnol. Biol. Med.* **2016**, *12*, 845−849.
(14) Wibroe, P. P.; Anselmo, A. C.; Nilsson, P. H.; Sarode, A.; Gupta, V.; Urbanics, R.; Szebeni, J.; Hunter, A. C.; Mitragotri, S.; Mollnes, T. E.; Moghimi, S. M. Bypassing adverse injection reactions to nanoparticles through shape modification and attachment to erythrocytes. *Nat. Nanotechnol.* **2017**, *12*, 589−594.
(15) Blicher, A.; Wodzinska, K.; Fidorra, M.; Winterhalter, M.; Heimburg, T. The temperature dependence of lipid membrane permeability, its quantized nature, and the influence of anesthetics. *Biophys. J.* **2009**, *96*, 4581−4591.
(16) Israelachvili, J. N. *Intermolecular and Surface Forces*, 3; Academic Press: San Diego, 2011.
(17) Marsh, D. *Handbook of Lipid Bilayers*, 2; CRC Press: Boca Raton, 2013.
(18) Marsh, D. Lateral pressure in membranes. *Biochim. Biophys. Acta* **1996**, *1286*, 183−223.
(19) Kaganer, V. M.; Möhwald, H.; Dutta, P. Structure and phase transitions in Langmuir monolayers. *Rev. Mod. Phys.* **1999**, *71*, 779−819.
(20) Kjaer, K.; Als-Nielsen, J.; Helm, C. A.; Laxhuber, L. A.; Möhwald, H. Ordering in Lipid Monolayers Studied by Synchrotron X-Ray Diffraction and Fluorescence Microscopy. *Phys. Rev. Lett.* **1987**, *58*, 2224−2227.
(21) Als-Nielsen, J.; Jacquemain, D.; Kjaer, K.; Leveiller, F.; Lahav, M.; Leiserowitz, L. Principles and applications of grazing incidence X-ray and neutron scattering from ordered molecular monolayers at the air-water interface. *Phys. Rep.* **1994**, *246*, 251−313.
(22) Kjaer, K. Some simple ideas on X-ray reflection and grazing-incidence diffraction from thin surfactant films. *Phys. B* **1994**, *198*, 100−109.
(23) Jensen, T. R.; Kjaer, K. Structural Properties and interactions of thin films at the air-liquid interface extrapolated by synchrotron X-ray Scattering. In *Novel Methods to Study Interfacial Layers*; Möbius, D., Miller, R., Eds.; Elsevier: Amsterdam, 2001; pp 205−254.
(24) Stefaniu, C.; Brezesinski, G. Grazing incidence X-ray diffraction studies of condensed double-chain phospholipid monolayers formed at the soft air/water interface. *Adv. Colloid Interface Sci.* **2014**, *207*, 265−279.
(25) Ishikawa, T.; Sakakibara, H.; Oiwa, K. The architecture of outer dynein arms in situ. *J. Mol. Biol.* **2007**, *368*, 1249−1258.
(26) Neuhaus, F.; Mueller, D.; Tanasescu, R.; Balog, S.; Ishikawa, T.; Brezesinski, G.; Zumbuehl, A. Vesicle Origami: Cuboid Phospholipid Vesicles Formed by Template-Free Self-Assembly. *Angew. Chem., Int. Ed.* **2017**, *56*, 6515−6518.
(27) Dubois, M.; Demé, B.; Gulik-Krzywicki, T.; Dedieu, J.-C.; Vautrin, C.; Désert, S.; Perez, E.; Zemb, T. Self-assembly of regular hollow icosahedra in salt-free catanionic solutions. *Nature* **2001**, *411*, 672−675.
(28) Kitaigorodskii, A. I. *Organic Chemical Crystallography*; Consultants Bureau: New York, 1961.
(29) Smith, E. A.; Dea, P. K. Differential Scanning Calorimetry Studies of Phospholipid Membranes: The Interdigitated Gel Phase. In *Applications of Calorimetry in a Wide Context—Differential Scanning Calorimetry, Isothermal Titration Calorimetry and Microcalorimetry*; Elkordy, A. A., Ed.; InTech: Rijeka, 2013.
(30) Mellal, D.; Zumbuehl, A. Exit-strategies—smart ways to release phospholipid vesicle cargo. *J. Mater. Chem. B* **2014**, *2*, 247−252.
(31) Sund-Levander, M.; Forsberg, C.; Wahren, L. K. Normal oral, rectal, tympanic and axillary body temperature in adult men and women: a systematic literature review. *Scand. J. Caring Sci.* **2002**, *16*, 122−128.